文章编号:1006-9941(2020)03-0182-08

6-((2*H*-tetrazol-5-yl)-amino)-1,2,4,5-tetrazin-3(2*H*)-one: High-nitrogen Insensitive Energetic Compound Stabilized by π-stacking and Hydrogen-bonding Interactions

ZHANG Cong[1], CHEN Xiang[1], BAI Yang[1], GUO Zhao-qi[1], SONG Ji-rong[2], MA Hai-xia[1]

(1. *School of Chemical Engineering, Northwest University, Xi'an*, 710069, *China*; 2. *Conservation Technology Department, the Palace Museum, Beijing* 100009, *China*.)

Abstract: 6-((2*H*-tetrazol-5-yl)-amino)-1,2,4,5-tetrazin-3(2*H*)-one (TATzO) was synthesized and characterized by FT-IR, elemental analysis, ^{1}H NMR and ^{13}C NMR and single crystal X-ray diffraction. The single crystal structure solution indicates that a hydrate forms (TATzO·H_2O) and it crystallizes in the orthorhombic *Pnma* space group with a density of 1.730 g·cm^{-3} at 296 K. The thermal behavior and thermal decomposition kinetic of TATzO·H_2O were studied by differential scanning calorimetry (DSC) and thermogravimetry-derivative thermogravimetry (TG-DTG) methods. The thermal decomposition peak temperature is determined to be 230.46°C, indicating a similar thermal stability to cyclotrimethylenetrinitramine (RDX). The apparent activation energies (E) and pre-exponential constant (A) of the compound are 169.03 kJ·mol^{-1} and 15.65 s^{-1}, respectively. The thermal ignition temperature (T_{be}) and the critical temperature of thermal explosion (T_{bp}) is 213.75℃ and 223.03℃, respectively. The enthalpy of formation was theoretically calculated by Gaussian 03, and the detonation velocity (D) and detonation pressure (p) were calculated by the Kamlet-Jacobs (K-J) equation. The obtained D and p are 7757m·s^{-1} and 25.74 GPa, respectively. The impact sensitivity is larger than 24 J.

Key words: energetic material; 6-((2*H*-tetrazol-5-yl)-amino)-1,2,4,5-tetrazin-3(2*H*)-one; crystal structure; thermal behavior; detonation properties

CLC number: TJ55; O64 **Document code**: A **DOI**: 10.11943/CJEM2019067

1 Introduction

The energetic materials (EMs) used at present are mainly nitro (—NO_2), nitrate (—ONO_2), and nitramine (—$NHNO_2$) containing compounds, such as 2,4,6-trinitrotoluene (TNT), Hexogeon (RDX) and Octagon (HMX). These materials, however, have drawbacks of sensitive to external stimulus, high toxicity and high environmental contamination during production. Herein, it is essential to exploit alternative environmentally friendly and insensitive energetic materials[1]. High-nitrogen heterocycle compounds, including tetrazine, tetrazole and triazole, exhibit excellent properties such as high positive heats of formation (HOF), high density, low sensitivity, good thermal stability, and releasing environment-friendly decomposition products [2-5]. The 1,2,4,5-tetrazine heterocycle with four nitrogen atoms in the six-member ring, is electron-deficient at positions 3 and 6, at which nucleophilic aromatic substitution is extremely easy to take place [6-7]. Therefore, the oxygen balance and density of tetrazine derivatives could be further improved by introducing various explosophores at these two positions.

As high nitrogen content heterocycles, 1,2,4,5-

Received Date: 2019-03-15; **Revised Date**: 2019-04-12

Published Online: 2019-09-02

Project Supported: Project Supported: National Natural Science Foundation of China (21673179, 21504067, 21543016), Natural Science Foundation of Shaanxi Province(2018MJ2057)

Biography: ZHANG Cong(1993-), female, synthesis of energetic materials. e-mail:1656706389@ qq.com

Corresponding author: MA Hai-xia (1974-), female, Professor, major in synthesis and property of energetic materials. e-mail: mahx@ nwu.edu.cn

引用本文:张聪,陈湘,白杨,等. 高氮钝感含能化合物6-((2*H*-四唑-5-基)-氨基)-1,2,4,5-四嗪-3(2*H*)-酮:π-堆积和氢键作用[J]. 含能材料,2020,28(3):182-189.

ZHANG Cong, CHEN Xiang, BAI Yang,et al. 6-((2*H*-tetrazol-5-yl)-amino)-1,2,4,5-tetrazin-3(2*H*)-one: High-nitrogen Insensitive Energetic Compound Stabilized by π-stacking and Hydrogen-bonding Interactions[J]. *Chinese Journal of Energetic Materials*(*Hanneng Cailiao*),2020,28(3):182-189.

tetrazine derivatives have shown great potential in the design of EMs and several related compounds have been reported. However, to the best of our knowledge, most of these studies focused on the synthesis and characterization of symmetrical tetrazine compounds [4-6]. The unsymmetrical 1,2,4,5-tetrazine derivatives, such as 3-amino-6-nitroamino-tetrazine (ANAT) and 3-(3,3′-dinitroazetidine)-6-(3,5-dimethylpyrazole)-tetrazine (DNAZTzDMP), also have high positive HOF, good thermal stability, excellent detonation performance and mechanical stability for the applications of EMs. Probably due to the need for more synthetic steps, the derivatives of unsymmetrical 1,2,4,5-tetrazine are seldom studied [8-9]. Therefore, it is worthy of taking effort to explore novel unsymmetrical 1,2,4,5-tetrazine based materials.

Hydrogen bonding interaction plays an important role in reducing sensitivity and increasing density of EMs. The introduction of hydrogen bonding donor and accepter to a main moiety is good strategy for design EMs. In addition, the crystal packing within a lattice has been shown a great influence on the sensitivity of EMs. Explosives that have parallel layers are generally low-sensitive to mechanical stimuli due to the ability of the layers to freely slide and disperse energy upon external stimuli [10-11]. A co-planar molecular structure combining with multiple hydrogen bonding interactions may result in insensitive EMs.

In view of the above considerations, we designed and synthesized a novel unsymmetrical tetrazine derivative 6-((2*H*-tetrazol-5-yl)amino)-1,2,4,5-tetrazin-3(2*H*)-one (TATzO) using BTATz (3,6-Bis(1H-1,2,3,4-tetrazol-5-yl-amino)-1,2,4,5-tetrazine) as a raw material. In the structure, three-NH act as hydrogen donors while unprotonated N atoms and ketone O atom act as hydrogen acceptors. The crystal structure and thermal behavior of TATzO were investigated by single crystal X-ray diffraction, DSC and TG-DTG. The thermal explosion critical temperature (T_{bp}) was also estimated to evaluate the thermal safety performance. Besides, the detonation properties, including the detonation velocity (D) and pressure (p), were calculated based on Kamlet-Jacobs (K-J) equation, and the impact sensitivity (IS) was determined.

2 Experimental Part

2.1 Experimental Measurements

3,6-bis(3,5-dimethylpyrazolyl)-1,2,4,5-tetrazine (BT) and 3,6-bis(1*H*-1,2,3,4-tetrazol-5-ylamino)-1,2,4,5-tetrazine was prepared according to the Ref[7]. Sodium hydroxide and hydrochloric acid were purchased from Aladdin and used without further purification.

IR spectra were determined using an IRAffinity-1S spectrometer with ATR (Shimadzu). Elemental analysis was performed on a VarioEL Ⅲ analyzer (Elementar Co). ^{1}H and ^{13}C NMR spectra were recorded on 600 MHz NMR spectrometer (Bruker) at 25 ℃, respectively. TG-DTG and DSC measurements were performed on SDT-Q600 (TA) and Q2000 (TA) apparatus under nitrogen atmosphere at a heating rate of 10 ℃ min^{-1} with the nitrogen flowing rate of 50 ml·min^{-1}. The HOF of the title compound was theoretically calculated using Gaussian 03 program package[12].

The impact sensitivity test was performed on a ZBL-B impact sensitivity instrument (Nachcn). The mass of drop hammer was 2.0 kg, and the sample mass for test was 30 mg.

2.2 Synthesis of TATzO

BTATz (0.9 g, 4 mmol) was immersed in 1.0 mol/L NaOH solution (5mL) for 10 h at 25 ℃with stirring. After that, the obtained solution was neutralized with 3 mol/L HCl aqueous solution until the bright orange precipitate formed. The precipitate was filtered, washed with H_2O and dried under vacuum to give TATzO as orange solid or powder (Scheme 1). Elemental analysis: calcd (%) for $C_3H_3N_9O$: C 19.82, H 1.84, N 70.21; found: C 19.89, H 1.67, N 69.90. IR (ATR, ν/cm^{-1}) 3498(w), 3433(w), 3252(m), 3184(m), 1693(s), 1573(s), 1514(s), 1406(s), 1357(m), 1155(m), 1103(s), 1043(s), 993(s). ^{1}H NMR(600 MHz, DMSO-d_6): δ 12.13(s,1H); ^{13}C NMR(600 MHz, DMSO-d_6): δ 151.2, 151.7, 155.6.

2.3 Crystal Structure Determination

The crystal of TATzO was chosen for X-ray de-

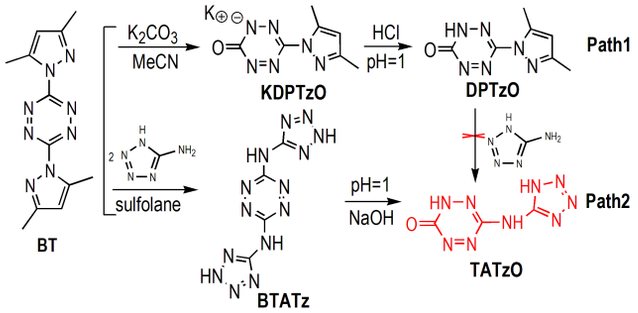

Scheme 1 Synthesis of TATzO

termination. The data were collected on a Bruker SMART APEX CCD X-ray diffractometer (Bruker, Germany) with graphite-monochromatized Mo-K_α radiation (λ = 0.071073 nm). The structure was solved by the direct methods and refined by the full-matrix least-squares method on F^2 with anisotropic thermal parameters for all nonhydrogen atoms (SHELXS-97 and SHELXL2014)[13-14]. The hydrogen positions for water molecules were calculated by Fourier syntheses and hydrogen atoms of TATzO were added to their geometrically ideal positions and refined isotropically using a riding model. Crystal data and refinement results were summarized in Table 1 (CCDC 1873209).

3 Results and Discussion

3.1 Synthesis of the Title Compound

We initially tried to prepare the target compound through path 1 (Scheme 1), and successfully obtained intermediate compound 6-(3,5-dimethylpyrazol-1-yl)-1,2,4,5-tetrazin-3(2*H*)-one(DPTzO)[15]. Then we attempted to synthesize TATzO involved the reaction of DPTzO and 5-amino-tetrazole(5-AT) in refluxing methanol. However, no product was obtained even after long reaction time. The reason was speculated to be that the strong electron-withdrawing effect of the ketone group reduces nucleophilic substitution ability of the para-carbon position of the tetrazine. After considering the reactivity of the tetrazine moiety, we switched the synthetic route to path 2 and successfully obtained the target compound.

3.2 Structural Characterization

It crystallizes with a calculated density of 1.730 g·cm^{-3} at 296 K in the orthorhombic *Pnma* space group. A water molecule co-crystallize in the single crystal so that the structure can be described as TATzO·H_2O (Fig.1). For the tetrazine and tetrazole rings, the N—C bond lengths are within the range between 1.276 Å to 1.410 Å and an average value of 1.351 Å, which is longer than normal N═C bond (1.22 Å) and shorter than normal N—C bond (1.47 Å) (Table 2). The N—N bond lengths have a minimum of 1.276 Å for N(1)—N(2) and a maximum of 1.355 Å for N(3)—N(4), which is longer than that of the normal N═N bond (1.20 Å) and

Table 1 X-ray diffraction data collection and refinement parameters for TATzO·H_2O

chemical formula	$C_3H_3N_9O\cdot H_2O$
M / g·mol^{-1}	199.16
crystal system	orthorhombic
space group	*Pnma*
V / Å^3	764.6(7)
Z	4
D_{calc} / g·cm^{-3}	1.730
F(000)	408.0
a / Å	14.217(8)
b / Å	6.209(3)
c / Å	8.662(5)
α / (°)	90.00
β / (°)	90.00
γ / (°)	90.00
θ / (°)	2.75−27.60
$R_{(int)}$	0.1098
goodness-of-fit on F^2	1.002
R indices ($I>2\sigma(I)$)	R_1=0.0603, wR_2=0.1279
R indices (all data)	R_1=0.1275 wR_2 = 0.1511
index ranges	$-18\leqslant h\leqslant 14$, $-6\leqslant k\leqslant 8$, $-11\leqslant l\leqslant 11$
reflections collected/unique	945/4147
T / K	296

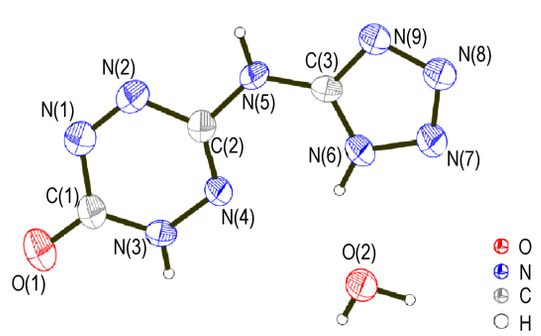

Fig.1 The asymmetric unit of TATzO·H_2O, with displacement ellipsoids drawn at the 30% probability level.

Table 2 Selected bond lengths and bond angles of TATzO·H_2O

bond	lengths / Å	bond	lengths / Å	bond	angles / (°)	bond	angles / (°)
O(1)—C(1)	1.228(5)	N(6)—N(7)	1.350(4)	N(2)—N(1)—C(1)	121.3(3)	N(4)—C(2)—N(5)	121.3(3)
N(1)—N(2)	1.276(6)	N(6)—C(3)	1.323(5)	N(1)—N(2)—C(2)	116.9(4)	N(5)—C(3)—N(6)	127.0(4)
N(1)—C(1)	1.410(6)	N(7)—N(8)	1.280(4)	N(4)—N(3)—C(1)	124.6(3)	N(5)—C(3)—N(9)	123.4(4)
N(2)—C(2)	1.390(5)	N(8)—N(9)	1.363(5)	N(3)—N(4)—C(2)	114.1(3)	N(6)—C(3)—N(9)	109.6(3)
N(3)—N(4)	1.355(4)	N(9)—C(3)	1.311(5)	C(2)—N(5)—C(3)	125.3(3)	O(1)—C(1)—N(1)	119.2(4)
N(3)—C(1)	1.339(5)	N(5)—C(2)	1.388(5)	N(7)—N(6)—C(3)	108.1(3)	O(1)—C(1)—N(3)	124.6(4)
N(4)—C(2)	1.279(5)	N(5)—C(3)	1.366(5)	N(6)—N(7)—N(8)	106.1(3)	N(1)—C(1)—N(3)	116.3(4)
				N(7)—N(8)—N(9)	111.4(3)	N(2)—C(2)—N(4)	126.8(4)
				N(8)—N(9)—C(3)	104.7(3)	N(2)—C(2)—N(5)	111.8(4)

shorter than that of the normal N—N bond (1.41 Å)[16]. The tetrazine ring and the tetrazole moiety connected by amino group located on a crystallographic mirror plane. Thus, the whole molecule is a plane structure. The TATzO and solvent molecules bring about six types of hydrogen bonds in the crystal(Table 3), including five intermolecular hydrogen bonds (O(2)—H(2)···N(9)^{i}, O(2)—H(2)A···N1^{ii}, N(3)—H(3)···N(8)^{i}, N(5)—H(5)···O(1)^{iii}, N(6)—H(6)···O(2)) and one intramolecular hydrogen bond (N(6)—H(6)···N(4)).

Table 3 Hydrogen-bond geometry of TATzO·H_2O

D—H···A	*d*(D—H)	*d*(H···A)/ Å	∠D—H···A / (°)	*d*(D···A) / Å
O(2)—H(2)A···N(1)^{ii}	0.860(19)	1.99(2)	176.0(5)	2.851(5)
O(2)—H(2)B···N(9)^{i}	0.842(19)	1.88(2)	170.0(5)	2.715(5)
N(3)—H(3)···N(8)^{i}	0.86	2.020	170.0	2.869(5)
N(5)—H(5)···O(1)^{iii}	0.86	2.130	173.3	2.986(4)
N(6)—H(6)···O(2)	0.86	1.860	141.1	2.588(5)
N(6)—H(6)···N(4)	0.86	2.250	118.0	2.759(4)

Note: Symmetry codes: (i) 0.5+*x*, 0.5-*y*, 0.5-*z*; (ii) *x*, *y*, −1+*z*; (iii) −0.5+*x*, 0.5-*y*, 1.5-*z*.

Besides, those hydrogen bonds also form hydrogen-bond graph-set motifs ($R_3^4(8)$, $R_2^3(10)$ and $R(6)$), according to the definition of Bernstein[17]. The extensive inter- and intramolecular hydrogen bonds link the molecules into two-dimensional layer like structure (Fig.2). It is reported that the intensive hydrogen-bonding interactions make an important contribution to improving the thermal stability and decreasing the sensitivity of EMs. On the other hand, the crystal structure of TATzO·H_2O features face-to-face geometries with the interlayer distance of 3.104 Å and the π-stacked sheets are arranged in a layer-like structure(Fig.3). In the case of external mechanical stimulation, the π-stacked structures can cause slippage between the layers, thereby counteracting external stimuli and reducing sensitivity.[18]

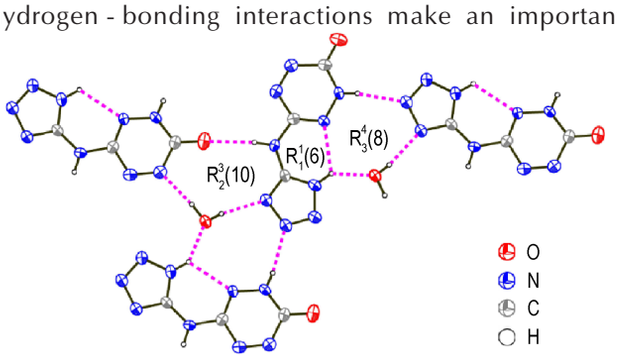

Fig. 2 The two-dimensional structure of TATzO·H_2O along the *b* axis hydrogen-bond interactions are shown as dashed lines.

To further understand the interactions between the molecules contained in TATzO·H_2O, the Hirshfeld surface and the 2D fingerprint spectrum were analyzed[19-21]. Fig.4 shows an approximately plate-like surface, indicating that the planar molecule of TATzO·H_2O. Besides, the red dots showing the intermolecular close contacts are located on the side faces of the plate. It suggests that the intermolecular interactions in the crystal occur through the oxygen

and nitrogen atoms encompassing the molecules. From fingerprint spectra of TATzO·H_2O in Fig. 5, it was observed that two sharp spikes exist in the bottom left of the spectra, indicating the interactions of O···H and N···H. Among them, the interaction of N···H (44.5%) was much higher than that of O···H (16.8%), showing the main interactions of the energetic molecules were N···H interactions.

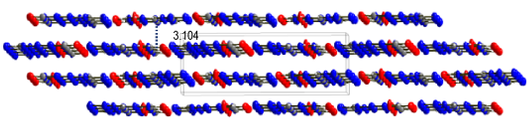

Fig. 3 Crystal packing of TATzO·H_2O along the *c* axis.

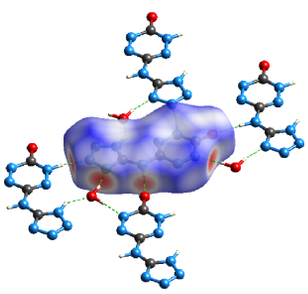

Fig.4 Hirshfeld surface of TATzO·H_2O.

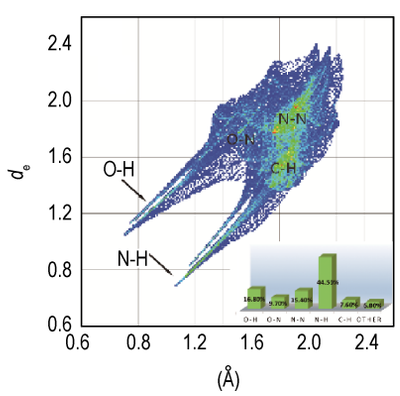

Fig.5 Fingerprint spectra of TATzO·H_2O.

3.3 Thermal Behavior Analysis

The typical DSC and TG-DTG curves of TATzO·H_2O measured at heating rate of 10.0 K·min^{-1} are shown in Fig. 6 and Fig. 7. Both DSC and TG-DTG curves show two reaction processes. On the DSC curve, the first stage is an endothermic decomposition process with the peak temperature of 136.34 ℃ due to the dehydration of crystalline water. The second one is an intense exothermic decomposition process with the peak temperature of 230.46 ℃, which is higher than 1,1-diamino-2,2-dinitroethylene FOX-7 (221.9 ℃) and lower than BTATz (320.5 ℃)[7,22]. Meanwhile, the first stage of decomposition process on TG curve between 129.18 to 138.94 ℃ with a mass loss of 9.14% corresponds to the releasing of crystalline water (cal: 9.05%). The second stage ranges from 213.59 ℃ to 234.05 ℃ with a mass loss of 35.49%.

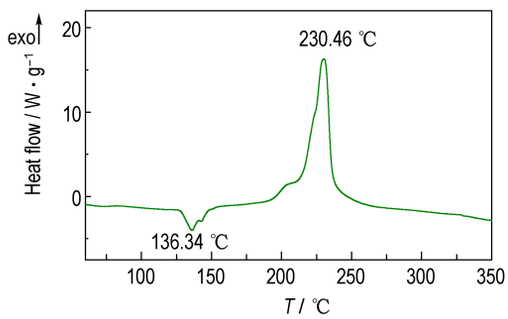

Fig.6 DSC curve for TATzO·H_2O at 10 ℃·min^{-1}

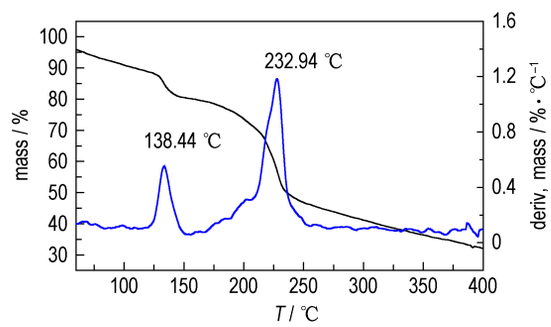

Fig.7 TG-DTG curves for TATzO·H_2O at 10 ℃·min^{-1}

3.4 Non-isothermal Kinetics and Thermal Explosion Critical Temperature

In order to estimate the thermal kinetics of the intense exothermic process of TATzO·H_2O during the decomposition process, the kinetic parameters (the apparent activation energy (E) and pre-exponential constant (A)) have been calculated through Kissinger method [23] and Ozawa method [24] at different T_p (maximum peak temperature) and T_e (the extrapolated onset temperature). All the data are listed in Table 4. The value of E_O obtained by Ozawa method is in agreement with E_K obtained by Kissinger method, and the linear correlation coefficient shows that the result is convincible.

Kissinger method:

$$\ln\frac{\beta}{T_p^2} = \ln\frac{AR}{E} - \frac{E}{RT_p} \quad (1)$$

Flynn-Wall-Ozawa method:

$$\lg\beta + \frac{0.4567E}{RT} = C \quad (2)$$

Table 4 The kinetic parameters for TATzO·H_2O at various heating rates.

β / ℃·min^{-1}	T_e / ℃	E_{Oe} / kJ·mol^{-1}	R^2_{Oe}	T_p / ℃	E_K / kJ·mol^{-1}	log(A_K / s^{-1})	R^2_K	E_O / kJ·mol^{-1}	R^2_O
5	211.91	157.005	0.9982	222.28	169.033	15.6549	0.9994	168.741	0.9994
10	219.21			230.46					
15	225.05			235.62					
20	227.81			239.23					
25	231.41			241.66					
30	234.05			243.54					

Note: β is heating rate; T_e is onset temperature in the DSC curve; T_p is maximum peak temperature; E_{Oe} is apparent activation energy calculated by Ozawa method using T_e; E_K is apparent activation energy calculated by Kissinger method; E_O is apparent activation energy calculated by Ozawa method using T_p; A_K is pre-exponential constant calculated by Kissinger Methed; R^2_{Oe}, R^2_K and R^2_O: linear correlation coefficient.

The thermal stability of the EMs can be evaluated through the thermal ignition temperature (T_{be}) and the thermal explosion critical temperature (T_{bp}). T_{be} and T_{bp} were obtained by third order polynomial fit of the extrapolated onset decomposition temperature (T_e) and the extrapolated peak temperature (T_p) corresponding to $\beta \rightarrow 0$ based on Eqs.(3) and (4)[26-27]. The parameters *a*, *b* and *c* are coefficients. The values of T_{be} and T_{bp} of the compound are 213.75 ℃and 223.03 ℃, respectively, which are higher than the typical explosive FOX-7(206.0, 207.1 ℃) and lower than BTATz (262.5, 272.1 ℃), indicating good thermal stability of the title compound [25]. We speculate that high thermal stability is caused by the presence of a conjugation in the molecular structure and the introduction of amino groups to the structure.

$$T_{e\,or\,p} = T_{e0\,or\,p0} + a\beta_i + b\beta_i^2 + b\beta_i^3 + b\beta_i^4,\ i = 1\sim6 \quad (3)$$

$$T_{be\,or\,bp} = \frac{E_{oe\,or\,op} - \sqrt{E_{oe\,or\,op} - 4E_{oe\,or\,op}RT_{oe\,or\,op}}}{2R} \quad (4)$$

3.5 Heats of Formation and Detonation Properties

The HOF of TATzO was calculated by designing an isodesmic reaction (Scheme 2). For the involved compounds, geometric optimization and frequency were calculated using the B3LYP functional with the 6-311+G** basis set and the HOF of C_2HN_4O (1,2,4,5-tetrazin-3(2*H*)-one) was obtained by G3 method. All of the optimized structures were characterized to be local energy minima on the potential-energy surface without any imaginary frequency. On the basis of the energy properties of the reference compounds (Table 5), the HOF of C_2HN_4O calculated by G3 theory is 459.92 kJ·mol^{-1}, and the HOF of TATzO was predicted to be 777.09 kJ·mol^{-1}.

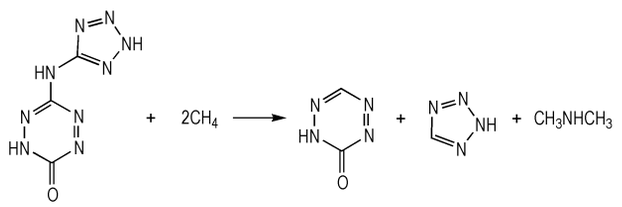

Scheme 2 Designed isodesmic reaction for the prediction of the HOF of TATzO.

Table 5 Total energies (E_0), zero-point energies (*ZPE*), thermal corrections(H_T), and HOFs

compound	E_0 / a.u.	*ZPE* / a.u.	H_T / a.u.	HOF / kJ·mol^{-1}
CH_4	−40.520993	0.0450	0.0038	−74.6[28]
CH_3NHCH_3	−135.161638	0.0922	0.0055	−22.5[28]
C_2HN_4O	−371.515587	0.0556	0.0061	459.9[29]
1*H*-tetrazole	−258.211462	0.0460	0.0044	326.0[1)]
TATzO	−683.896275	0.0995	0.0106	777.1

Note: 1) HOF by G3 (kJ·mol^{-1}).

Then, the heat of formation of TATzO (677.8 kJ·mol^{-1}) in solid state was estimated with Trouton's rule (Eq. 5), in which T_d represents the decomposition temperature [30].

$$\Delta H_f(s) = \Delta H_f(g) + \Delta H_{sub} = \Delta H_f(g) - 188 \times T_d \quad (5)$$

The performance of EMs is evaluated by its detonation velocity (D) and detonation pressure (p). And the empirical Kamlet-Jacobs (K-J) equation (Eqs.(6)−(8)) are widely applied to estimate the values of D and p for the explosives containing C, H, O, and N as follows[31]:

$$D = 1.01(NM_{ave}1/2Q^{1/2})^{1/2}(1 + 1.30\rho) \quad (6)$$

$$p = 1.558\rho^2 NM_{ave}1/2Q^{1/2} \quad (7)$$

$$Q = \frac{-[\Delta H_f(\text{detonation product uction}) - \Delta H_f(\text{energetic complex})]}{\text{formula mass of energetic complex}} \quad (8)$$

where D is detonation velocity ($m\cdot s^{-1}$), p is detonation pressure (GPa), N is moles of gaseous detonation products per gram of explosives, M_{ave} is average molecular weights of gaseous products, Q is chemical energy of detonation ($J\cdot g^{-1}$), and ρ is the density of explosive ($g\cdot cm^{-3}$).

When using K-J equation, for the compound of $C_aH_bN_cO_d$, TATzO ($C_3H_3N_9O$) suites $b/2\geqslant c$, thus, the equation of explosion reaction is Equation (9):

$$C_3H_3ON_9 \rightarrow H_2O + (3/2-1)H_2 + 3C + 9/2N_2 + Q \quad (9)$$

Where $\Delta_f H_m^{\ominus}(H_2O, l) = -241.8\ kJ\cdot mol^{-1}$,

$\Delta_f H_m^{\ominus}(H_2, g) = 0\ kJ\cdot mol^{-1}$,

$\Delta_f H_m^{\ominus}(N_2, g) = 0\ kJ\cdot mol^{-1}$,

$\Delta_f H_m^{\ominus}(C, s) = 0\ kJ\cdot mol^{-1}$.

The calculated density of TATzO is 1.71 $g\cdot cm^{-3}$ by the Monte Carlo method, which is almost equal with the density of single crystal of $TATzO\cdot H_2O$. Consequently, the calculated Q, D and p are 5082 $J\cdot g^{-1}$, 7757 $m\cdot s^{-1}$ and 25.74 GPa, respectively. The detonation parameters of TATzO are slightly lower than those of BTATz (8055 $m\cdot s^{-1}$, 25.39 GPa)[7].

3.6 Impact Sensitivity

Sensitivity is an important property for EMs in terms of storage and practical application. The impact sensitivity (IS) was determined by fall hammer method using 2-kg drop weight with maximum height of 120 cm. No explosion was detected after 10 time strikes which means the compound has the IS value larger than 24 J. The IS of TATzO is slightly lower than BTATZ (22 J). The reason for the low sensitivity is that there are hydrogen bonds and π stacking in the crystal. The π stacking in crystal makes it impossible to slide the molecules during impact resistance, resulting in counteracting external stimuli and reducing sensitivity [32].

4 Conclusions

(1) The unsymmetrical tetrazine derivative 6-((2*H*-tetrazol-5-yl)-amino)-1,2,4,5-tetrazin-3(2*H*)-one (TATzO) was synthesized and characterized by IR, EA and NMR. The hydrate with composition of $TATzO\cdot H_2O$ was confirmed by single crystal analysis. The adjacent molecules form face-to-face molecular packing diagram with the interlayer distance of 3.104 Å. The π-stacked sheets are further expanding into layer-like structure through intensive hydrogen-bonding interactions.

(2) The thermal decomposition peak temperature is determined to be 230.46 ℃, indicating a better thermal stability than the traditional explosive FOX-7. The detonation velocity (D) and pressure (p) estimated by Eq. of Kamlet-Jacobs (K-J) are 7757 $m\cdot s^{-1}$ and 25.74 GPa, respectively.

References:

[1] Wang B, Qi X, Zhang W, et al. Synthesis of 1-(2H-tetrazol-5-yl)-5-nitraminotetrazole and its derivatives from 5-aminotetrazole and cyanogen azide: a promising strategy towards the development of C—N linked bistetrazolate energetic materials [J]. *Journal of Materials Chemistry A*, 2017, 5(39): 20867−20873.

[2] Tang Y, Kumar D, Shreeve J M. Balancing excellent performance and high thermal stability in a dinitropyrazole fused 1, 2, 3, 4-Tetrazine[J]. *Journal of the American Chemical Society*, 2017, 139(39): 13684−13687.

[3] Chand D, Damon A P, Shreeve J M. Di(1*H*-tetrazol-5-yl)methanone oxime and 5, 5′-(hydrazonomethylene) bis(1*H*-tetrazole) and their salts: a family of highly useful new tetrazoles and energetic materials[J]. *Journal of Materials Chemistry A*, 2013, 1(48): 15383−15389.

[4] Qu Y Y, Babailov S P. Azo-linked high-nitrogen energetic materials[J]. *Journal of Materials Chemistry A*, 2018, 6(5):1915−1940.

[5] Pagoria P F, Lee G S, Mitchell AR, et al. Pagoria, et al. A review of energetic materials synthesis [J]. *Thermochimica Acta*, 2002, 384(1):187−204.

[6] Chavez D E, Hiskey M A, Gilardi R D. Novel high-nitrogen materials based on nitroguanyl-substituted tetrazines[J]. *Organic Letters*, 2004, 6(17): 2889−2891.

[7] Saikia A, Sivabalan R, Polke B G, et al. Synthesis and characterization of 3, 6-bis(1*H*-1, 2, 3, 4-tetrazol-5-ylamino)-1, 2, 4, 5-tetrazine (BTATz): Novel high-nitrogen content insensitive high energy material [J]. *Journal of hazardous materials*, 2009, 170(1): 306−313.

[8] Gao H, Wang R, Twamley B, et al. 3-Amino-6-nitroamino-tetrazine (ANAT)-based energetic salts.[J]. *Chemical Communications*, 2006, 38: 4007−4009.

[9] Myers T W, Chavez D E, Hanson S K, et al. Independent control of optical and explosive properties: pyrazole-tetrazine complexes of first row transition metals[J]. *Inorganic Chemistry*, 2015, 54(16): 8077−8086.

[10] Shlomovich A, Pechersky T, Cohen A, et al. Energetic isomers of 1, 2, 4, 5-tetrazine-bis-1, 2, 4-triazoles with low toxicity[J]. *Dalton Transactions*, 2017, 46(18): 5994−6002.

[11] Wang Y, Liu Y, Song S, et al. Accelerating the discovery of insensitive high-energy-density materials by a materials genome approach[J]. *Nature Communications*, 2018, 9(1): 2444−2455.

[12] Frisch M J, Trucks G W, Schlegel H B, et al. Gaussian 98, revision A.07 [CP]. Gaussian, Inc, Pittsburgh PA, 1998

[13] Sheldrick G M. SHELXTL-97, Structure Program for Crystal Structure Solution [CP]. University of Göttingen, Göttingen, Germany. 1997.
[14] Sheldrick G M. SHELXTL-97, Structure Program for Crystal Structure Refinement [CP]. University of Göttingen, Göttingen, Germany. 1997.
[15] Ishmetova R, Latosh I, Ganebnykh N I, et al. Replacement of dimethyl-pyrazolyl group in 1,2,4,5-tetrazines by aliphatic alcohols and water[J]. *Russian Journal of Organic Chemistry*, 2009, 45(7):1102-1107.
[16] Zhang Z, Zhang J. 1-Amine-1,2,3-triazolium salts with oxidizing anions: A new family of energetic materials with good performance [J]. *Journal of Molecular Structure*, 2018, 1158: 88-95.
[17] Bernstein J, Davis R E. Patterns in hydrogen bonding: functionality and graph set analysis in crystals[J]. *Angewandte Chemie International Edition*, 1995, 34:1555-1573.
[18] Zhang J, Zhang Q, Vo T T, et al. Energetic Salts with π-Stacking and Hydrogen-Bonding Interactions Lead the Way to Future Energetic Materials[J]. *Journal of the American Chemical Society*, 2015, 137(4):1697-1704.
[19] Spackman M A, Byrom P G. A novel definition of a molecule in a crystal[J]. *Chemical Physics Letters*, 1997, 267(3-4): 215-220.
[20] Spackman M A, McKinnon J J. Fingerprinting intermolecular interactions in molecular crystals[J]. *Cryst Eng Comm*, 2002, 4(66):378-392.
[21] Mckinnon J J, Jayatilaka D, Spackman M A. Towards quantitative analysis of intermolecular interactions with Hirshfeld surfaces[J]. *Chemical Communications*, 2007, 37:3814-3816.
[22] Anniyappan M, Talawar M B, Gore G M. et al. Synthesis, characterization and thermolysis of 1,1-diamino-2,2-dinitroethylene (FOX-7) and its salts [J]. *Journal of Hazardous Materials*, 2006, 137(2):812-819.
[23] Kissinger H E. Reaction Kinetics in Differential Thermal Analysis[J]. *Analytical Chemistry*, 1957, 29(11):1702-1706.
[24] Ozawa T B.A new method of analyzing thermogravimetric data [J] *Bulletin of the Chemical Society of Japan*, 1965, 38(11): 1881-1886.
[25] Qiu Q, Xu K, Yang S, et al. Syntheses and characterizations of two new energetic copper-amine-DNANT complexes and their effects on thermal decomposition of RDX[J]. *Journal of Solid State Chemistry*, 2013, 205:205-210.
[26] Ma H X, Yan B, Li Z N, et al. Synthesis, molecular structure, non-isothermal decomposition kinetics and adiabatic time to explosion of 3,3-dinitroazetidinium 3,5-dinitrosalicylate[J]. *Journal of Thermal Analysis and Calorimetry*, 2009, 95(2): 437-444.
[27] Hu, R, Yang Z, Liang Y. The determination of the most probable mechanism function and three kinetic parameters of exothermic decomposition reaction of energetic materials by a single non-isothermal DSC curve [J]. *Thermochimica Acta*, 1988, 123:135-151.
[28] Sil M, Gorai P, Das A, et al. Chemical modeling for predicting the abundances of certain aldimines and amines in hot cores [J]. *Astrophysical Journal*, 2017, 853(2): 139-159.
[29] Srinivas D, Ghule V D, Muralidharan K. Synthesis of nitrogen-rich imidazole, 1,2,4-triazole and tetrazole-based compounds [J]. *RSC Advances*, 2015, 45: 7041-7046.
[30] Searle M S, Wales D J, Williams D H, et al. Empirical Correlations between Thermodynamic Properties and Intermolecular Forces[J]. *Journal of the American Chemical Society*, 1995, 117(18): 5013-5015.
[31] Kamlet M J, Jacobs S J. Chemistry of Detonations. I. A Simple Method for Calculating Detonation Properties of C-H-N-O Explosives[J]. *Journal of Chemical Physics*, 1968, 48(1): 23-35.
[32] Ma Y U, Zhang A, Xue X, et al. Crystal Packing of Impact-Sensitive High-Energy Explosives [J]. *Crystal Growth & Design*, 2014, 14(11): 6101-6114.

高氮钝感含能化合物6-((2*H*-四唑-5-基)-氨基)-1,2,4,5-四嗪-3(2*H*)-酮:π-堆积和氢键作用

张 聪[1],陈 湘[1],白 杨[1],郭兆琦[1],宋纪蓉[2],马海霞[1]
(1. 西北大学化工学院,陕西 西安 710069; 2. 故宫博物院,北京 100009)

摘 要: 合成了6-((2*H*-四唑-5-基)-氨基)-1,2,4,5-四嗪-3(2*H*)-酮(TATzO)并通过红外光谱、元素分析、核磁和单晶X射线衍射对其结构进行了表征。单晶结构表明,TATzO·H_2O属于正交晶系,空间群是P*nma*,密度为1.730 g·cm^{-3}。在非等温条件下,利用差示扫描量热法(DSC)和热重(TG-DTG)研究了TATzO的热分解行为并计算得到分解峰温、活化能(*E*)、指前因子(*A*)、热点火温度(T_{be})和热爆炸临界温度(T_{bp}),分别为230.46 ℃、169.03 kJ·mol^{-1}、15.65 s^{-1}、213.75 ℃和223.03 ℃。TATzO·H_2O分解峰温和热爆炸临界温度与传统含能材料RDX相近,表明TATzO热稳定性较高。通过高斯03软件包设计等键反应计算生成焓(HOF),由Kamlet-Jacobs(K-J)方程计算爆速(*D*)和爆压(*p*)以评估爆轰性能。*D*和*p*分别为7757 m·s^{-1}和25.74 GPa。落锤法测得TATzO撞击感度大于24 J。

关键词: 含能材料;6-((2*H*-四唑-5-基)-氨基)-1,2,4,5-四嗪-3-(2*H*)-酮;晶体结构;热行为;爆轰性能
中图分类号: TJ55; O64 **文献标志码:** A **DOI:**10.11943/CJEM2019067
(责编:王艳秀)